Coupled Systems Mechanics, *Vol. 11, No. 3 (2022) 217-231*
https://doi.org/10.12989/csm.2022.11.3.217

Multilayered frame structure subjected to non-linear creep: A delamination analysis

Victor I. Rizov*[1] and Holm Altenbach[2]

[1]Department of Technical Mechanics, University of Architecture, Civil Engineering and Geodesy, 1 Chr. Smirnensky Blvd., 1046 - Sofia, Bulgaria
[2]Lehrstuhl für Technische Mechanik, Fakultät für Maschinenbau, Otto-von-Guericke-Universität Magdeburg, Universitätsplatz 2, 39106 Magdeburg, Deutschland

(Received November 12, 2021, Revised December 21, 2021, Accepted January 5, 2022)

Abstract. The present paper is concerned with a delamination analysis of a multilayered frame structure that exhibits non-linear creep behavior. A solution to the strain energy release rate is obtained by considering the time-dependent complementary strain energy in the frame. The mechanical behavior of the frame is treated by using a non-linear stress-strain-time relationship. The time-dependent solution to the strain energy release rate obtained in the present paper holds for a multilayered frame made of arbitrary number of adhesively bonded layers of different thicknesses and material properties. Besides, the dealamination is located arbitrary along the thickness. The solution to the strain energy release rate is verified by applying the *J*-integral approach. A parametric study of the strain energy release rate is carried-out. Two three-layered frame configurations are analyzed in order to evaluate the influence of the delamination crack location along the thickness on the strain energy release rate. The strain energy release is analyzed also for the case when a notch is cut-out in the inner delamination crack arm. The results obtained are compared with these for a frame without a notch.

Keywords: delamination; frame structure; multilayered material; non-linear creep; notch

1. Introduction

Multilayered materials consist of adhesively bonded layers of different materials. Multilayered materials have numerous applications in modern engineering (Amenzadeh *et al.* 2006, Amenzadeh and Kiyasbeyli 2007, Amenzadeh *et al.* 2011, Araki *et al.* 1992, Cilli and Ozturk 2010, Katsuhiko Ariga *et al.* 2012, Kaul 2014, Lloyd and Molina-Aldareguia 2003, Şansveren and Yaman 2019, Ozturk 2017, Ozturk and Akbarov 2009, Shestov *et al.* 2017, Maraş *et al.* 2018, Maraş *et al.* 2019, Tekalur *et al.* 2008, Tench and White 1991, Wang *et al.* 2019). For example, the extensive use of multilayered materials and structural components in many applications in aeronautics, automotive industry and civil engineering is due mainly to the higher strength-to-weight and stiffness-to-weight ratios of multilayered materials in comparison to the conventional homogeneous structural materials. The multilayered materials are exceptionally appropriate for building-up of lightweight

*Corresponding author, Professor, E-mail: V_RIZOV_FHE@UACG.BG
[a]Professor, E-mail: holm.altenbach@ovgu.de

http://www.techno-press.org/?journal=csm&subpage=8 ISSN: 2234-2184 (Print), 2234-2192 (Online)

structures in engineering applications where the low weight is of primary concern. However, the multilayered materials and structures have relatively low transversal strength in tension. This fact makes the multilayered structural members very vulnerable to delamination cracking. Actually, the delamination or separation of layers is the predominant failure mode in multilayered structures. Therefore, various aspects of the delamination phenomenon have to be analyzed in order to improve the delamination behavior of multilayered materials. The delamination has been analyzed mainly assuming linear-elastic behavior of the layered material. Recently, works on delamination in multilayered beam configurations, which show also nonlinear elastic behavior, published (Rizov 2017, Rizov 2018, Rizov 2019, Rizov and Altenbach 2020, Rizov 2020, Rizov 2020, Rizov 2021).

In contrast to delamination analyses of multilayered beams developed in Rizov (2020, 2020a, 2021), the present paper deals with delamination in a multilayered frame structure. Besides, the present paper investigates the influence of the non-linear creep behavior of the multilayered material on the delamination in contrast to Rizov (2021) where the delamination has been analyzed for the case of beams exhibiting linear creep. Also, the delamination analyzed here is located entirely inside the frame structure in contrast to Rizov (2020, 2020a, 2021), where the delamination is located at the edge of the beam. The fact that the delamination is located inside the structure imposes the multilayered frame to be treated as a statically undetermined structure in order to determine the bending moments in the delamination crack arms which are needed to calculate the strain energy release rate. The solution to the strain energy release rate derived in the present paper takes into account the time-dependent delamination behavior of the frame induced by the non-linear creep. The delamination in the multilayered frame is analyzed also by applying the J-integral approach in order to verify the solution to the strain energy release rate.

2. Analysis of the strain energy release rate for delamination in multilayered frame

The multilayered frame depicted in Fig. 1 is under consideration. The frame consists of three multilayered bars AC, CR and RH. The length of each of the bars is l. The inclined bar AC, and the horizontal bar CR, are rigidly attached at C. The vertical bar RH is rigidly attached to the horizontal bar CR at R. Each of the bars has a rectangular cross-section of width b, and thickness h. The frame is supported by a rigid support in section A, and by a moveable support in section H, as shown in Fig. 1. The external loading consists of a bending moment M, applied in R. Apparently, in sections AC and CR, the frame is subjected to pure bending. Section RH of the frame is free of stresses (Fig. 1). It should be noted that the frame is made of an arbitrary number of adhesively bonded homogeneous layers. Besides, each of the layers has individual thickness and material properties. A delamination crack, LS, is located symmetrically with respect to C as shown in Fig. 1. The thicknesses of the inner and outer crack arms are h_1 and h_2, respectively. The delamination crack length is $2a$.

In each of the layers, the material exhibits non-linear creep behavior that is treated here by applying the following non-linear stress-strain-time relationship (Dowling 2013)

$$\varepsilon = \frac{\sigma_i}{E_i} + B_i \sigma_i^{m_i} t + D_i \sigma_i^{\alpha_i} \left(1 - e^{-\beta_i t}\right), \tag{1}$$

where ε is the strain, σ_i and E_i are, respectively, the stress and the modulus of elasticity in the i-th layer, B_i, m_i, D_i, α_i and β_i are material parameters in the i-th layer, t is the time. It should be mentioned

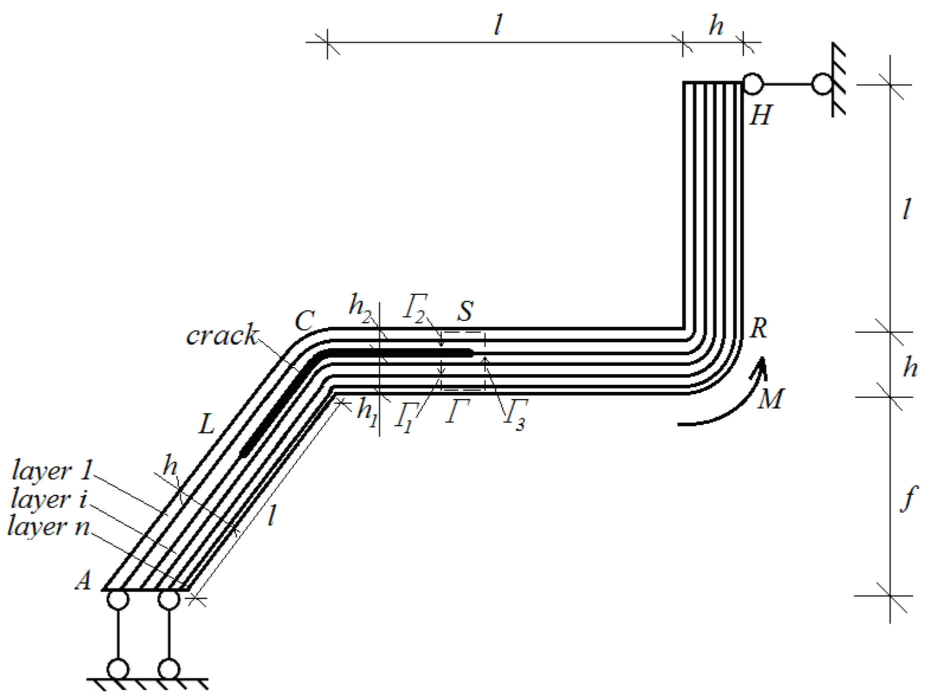

Fig. 1 Geometry and loading of a multilayered frame configuration with a delamination crack

that the first term of the right-hand side of Eq. (1) describes the instantaneous linear-elastic strain. The creep strain is described by the second and the third terms of the right-hand side of (1).

The main goal of the present paper is to derive a solution to the strain energy release rate for the delamination crack in the multilayered frame with considering the non-linear creep behavior. Due to the symmetry, only section, *CR*, of the frame is analyzed. The strain energy release rate, *G*, is written as (Rizov 2020)

$$G = 2\frac{dU^*}{bda}, \tag{2}$$

where U^* is the complimentary strain energy cumulated in portion, *CR*, of the frame, *da* is an elementary increase of the delamination crack length. It should be noted that the right-hand side of (2) is doubled in view of the symmetry (Fig. 1).

The complementary strain energy cumulated in section, *CR*, of the frame is expressed as

$$U^* = U_1^* + U_2^* + U_3^*, \tag{3}$$

where U_1^*, U_2^* and U_3^* are the complementary strain energy cumulated in the inner and outer crack arms, and in the un-cracked part of *CR*, respectively.

The complementary strain energy cumulated in the inner crack arm is obtained as

$$U_1^* = a\sum_{i=1}^{i=n_1} \iint_{(A_i)} u_{01i}^* dA, \tag{4}$$

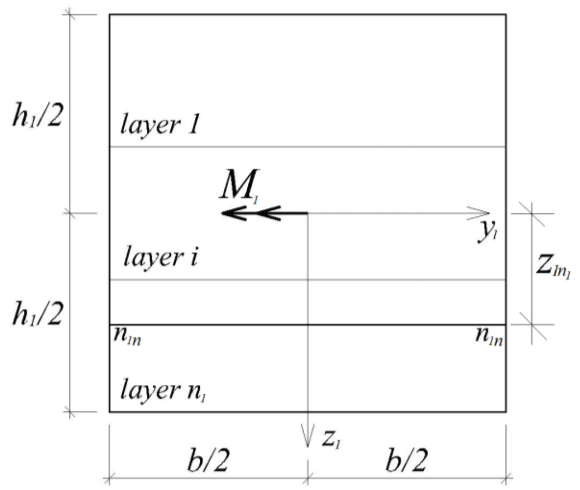

Fig. 2 Cross-section of the inner crack arm (the position of the neutral axis is marked by n_{1n}–n_{1n})

where n_1 is the number of layers in the inner crack arm, A_i is the area of the cross-section of the i-th layer and u^*_{01i} is the complementary strain energy density in the same layer.

The following formula is applied to obtain the complementary strain energy density (Rizov 2020)

$$u^*_{01i} = \sigma_{1i}\varepsilon - u_{01i}\,, \tag{5}$$

where σ_{1i} is the stress and u_{01i} is the strain energy density in the i-th layer. Since the strain energy density is equal to the area enclosed by the stress-strain curve, u_{01i} is written as

$$u_{01i} = \int_0^{\varepsilon} \sigma_{1i} d\varepsilon\,. \tag{6}$$

By combining of (1) and (6), the strain energy density is obtained as

$$u_{01i} = \frac{\sigma_i^2}{2E_i} + \frac{B_i m_i \sigma_i^{m_i+1} t}{m_i+1} + \frac{D_i \alpha_i \sigma_i^{\alpha_i+1}}{\alpha_i+1}\left(1-e^{-\beta_i t}\right)\,. \tag{7}$$

By substituting of (1) and (7) in (5), one derives

$$u^*_{01i} = \frac{\sigma_i^2}{2E_i} + \frac{B_i \sigma_i^{m_i+1} t}{m_i+1} + \frac{D_i \sigma_i^{\alpha_i+1}}{\alpha_i+1}\left(1-e^{-\beta_i t}\right). \tag{8}$$

The distribution of the strains which are involved in (1) is treated here by applying the Bernoulli's hypotheses for plane sections. First, the distribution of strains along the thickness of the lower crack arm cross-section is written as

$$\varepsilon = \kappa_1\left(z_1 - z_{1n_1}\right), \tag{9}$$

where κ_1 is the curvature, z_{1n_1} is the coordinate of the neutral axis. Here, the neutral axis, n_{1n}–n_{1n}, shifts from the centroid because the beam is multilayered (Fig. 2). It should be noted that since frame sections, AC and CR, are subjected to pure bending, from the small strain compatibility equations it follows that ε is distributed linearly along the thickness of the cross-section.

The complementary strain energy in the outer crack arm is obtained as

$$U_2^* = a\sum_{i=1}^{i=n_2} \iint_{(A_i)} u_{02i}^* dA, \tag{10}$$

where n_2 is the number of layers in the outer crack arm, A_i is the area of the cross-section of the i-th layer and u_{02i}^* is the complementary strain energy density in the same layer. Formula (8) is applied to obtain u_{02i}^*. For this purpose σ_{1i} is replaced with σ_{2i}. Here, σ_{2i} is the stress in the i-th layer of the outer crack arm. Formula (9) is used to obtain the distribution of strains along the thickness of the outer crack arm. For this purpose, κ_1 and z_{1n_1} are replaced with κ_2 and z_{2n_2}, respectively. Here, κ_2 and z_{2n_2} are, respectively, the curvature and the neutral axis coordinate in the cross-section of the outer crack arm.

The quantities κ_1, z_{1n_1}, κ_2 and z_{2n_2}, are determined in the following way. First, the equation for equilibrium of the cross-section of the inner crack arm are written as

$$N_1 = \sum_{i=1}^{i=n_1} \iint_{(A_i)} \sigma_{1i} dA, \tag{11}$$

$$M_1 = \sum_{i=1}^{i=n_1} \iint_{(A_i)} \sigma_{1i} z_1 dA, \tag{12}$$

where N_1 and M_1 are, respectively, the axial force and the bending moment in the inner crack arm where $N_1=0$. The equations for equilibrium of the cross-section of the outer crack arm are expressed as

$$N_2 = \sum_{i=1}^{i=n_2} \iint_{(A_i)} \sigma_{2i} dA, \tag{13}$$

$$M_2 = \sum_{i=1}^{i=n_2} \iint_{(A_i)} \sigma_{2i} z_2 dA, \tag{14}$$

where N_2 and M_2 are, respectively, the axial force and the bending moment in the outer crack arm. Here, $N_2=0$.

Further, the equation for equilibrium of the bending moments is written as

$$M_1 + M_2 = M. \tag{15}$$

Finally, one equation is composed by treating the frame as an internally statically undetermined structure with one degree of indeterminacy (M_1 is taken as a redundant). The static indeterminacy is resolved by applying the theorem of Castigliano for structures exhibiting material non-linearity

$$\frac{dU_{CS}^*}{dM_1} = 0, \tag{16}$$

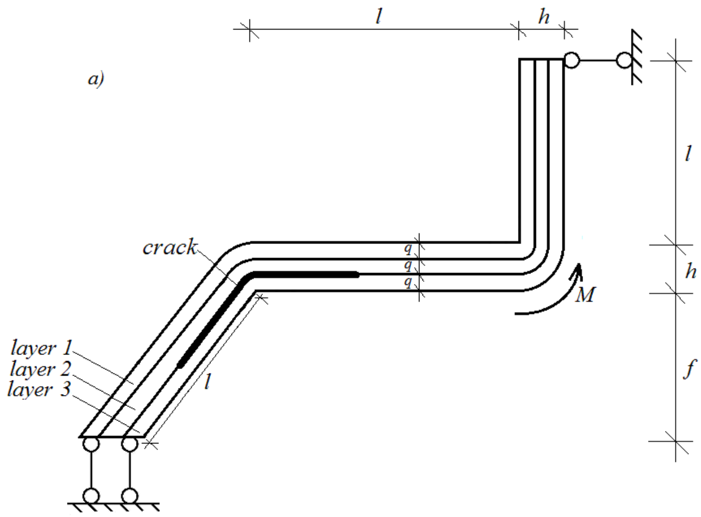

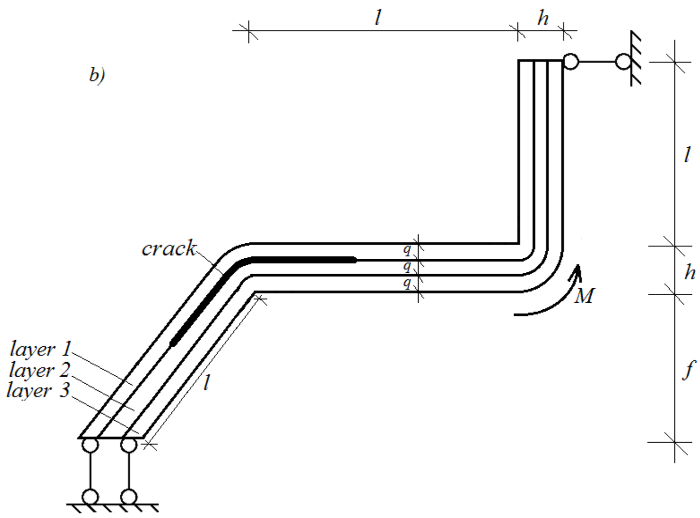

Fig. 3 Two three-layered frame configurations with a delamination crack located (a) between layers 2 and 3, and (b) between layers 1 and 2

where U^*_{CS} is the complementary strain energy in section, *CS*, of the frame (Fig. 1). It should be noted that the complementary strain energy in the un-cracked section, *SM*, does not depend on M_1. Thus, only the complementary strain energy in section, *CS*, of the frame is involved in (16). That is why, U^*_{CS} is found as

$$U^*_{CS} = U^*_1 + U^*_2 . \tag{17}$$

Eqs. (11)-(16) are solved with respect to M_1, M_2, κ_1, z_{1n_1}, κ_2 and z_{2n_2} by using the MatLab computer program at various values of time.

The complementary strain energy cumulated in the un-cracked part of *CR* is expressed as

$$U_3^* = (l-a)\sum_{i=1}^{i=n} \iint_{(A_i)} u_{03i}^* dA, \tag{18}$$

where n is the number of layers in the frame, u_{03i}^* is the complementary strain energy density in the i-th layer. The complementary strain energy, u_{03i}^*, is found by replacing of σ_{1i} with σ_{3i} in Eq. (8).

By substituting of (3), (4), (10) and (18) in (2), one derives the following solution to the strain energy release rate for the delamination crack in the multilayered frame shown in Fig. 1

$$G = \frac{2}{b}\left(\sum_{i=1}^{i=n_1} \iint_{(A_i)} u_{01i}^* dA + \sum_{i=1}^{i=n_2} \iint_{(A_i)} u_{02i}^* dA - \sum_{i=1}^{i=n} \iint_{(A_i)} u_{03i}^* dA \right). \tag{19}$$

The integration in (19) is carried-out by using the MatLab computer program. It should be mentioned that (19) can be applied to evaluate the creep induced time-dependent delamination behaviour of the frame since the complementary strain energy densities are functions of the time (refer to Eq. (8)).

The delamination in the multilayered frame is analyzed also by applying the *J*-integral approach in order to verify the solution to the strain energy release rate (Broek 1982). The *J*-integral is solved along the contour of integration, Γ, shown by a dashed line in Fig. 1. The solution to the *J*-integral is written as

$$J = 2\left(J_{\Gamma_1} + J_{\Gamma_2} + J_{\Gamma_3}\right), \tag{20}$$

where J_{Γ_1}, J_{Γ_2} and J_{Γ_3} are the values of the *J*-integral in segments Γ_1, Γ_2 and Γ_3, of the integration contour, respectively. Segments Γ_1, Γ_2 and Γ_3, coincide with the cross-sections of the inner and the outer crack arms and with the un-cracked part of section, *CR*, respectively. It should be mentioned that the expression in brackets in Eq. (20) is doubled in view of the symmetry (Fig. 1).

In segment, Γ_1, of the integration contour, the *J*-integral is expressed as

$$J_{\Gamma_1} = \sum_{i=1}^{i=n_1} \int_{s_{1i}} \left[u_{01i}\cos\alpha_{\Gamma_1} - \left(p_{x_{1i}} \frac{\partial u}{\partial x_{\Gamma_1}} + p_{y_{1i}} \frac{\partial v}{\partial x_{\Gamma_1}} \right) \right] ds_{\Gamma_1}, \tag{21}$$

where α_{Γ_1} is the angle between the outwards normal vector to the contour of integration and the crack direction, $p_{x_{1i}}$ and $p_{y_{1i}}$ are the horizontal and vertical components of the stress vector, u and v are the horizontal and vertical components of the displacement vector, and ds_{Γ_1} is a differential element along the contour of integration.

The components of (21) are obtained as

$$p_{x_{1i}} = -\sigma_{1i}, \tag{22}$$

$$p_{y_{1i}} = 0, \tag{23}$$

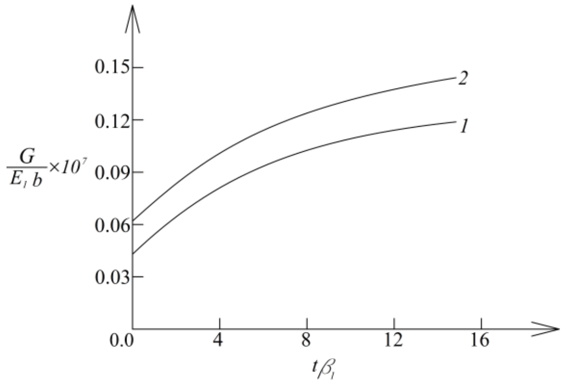

Fig. 4 The strain energy release rate in non-dimensional form plotted against the non-dimensional time (curve 1 - for the three-layered frame configuration with a delamination between layers 1 and 2, and curve 2 - for the three-layered frame configuration with a delamination between layers 2 and 3)

$$ds_{\Gamma_1} = dz_1, \tag{24}$$

$$\cos\alpha_{\Gamma_1} = -1, \tag{25}$$

$$\frac{\partial u}{\partial x_{\Gamma_1}} = \varepsilon = \kappa_1 \left(z_1 - z_{1n_1}\right). \tag{26}$$

The J-integral in segment, Γ_2, of the integration contour is written as

$$J_{\Gamma_2} = \sum_{i=1}^{i=n_2} \int_{s_{2i}} \left[u_{02i} \cos\alpha_{\Gamma_2} - \left(p_{x_{2i}} \frac{\partial u}{\partial x}_{\Gamma_2} + p_{y_{2i}} \frac{\partial v}{\partial x_{\Gamma_2}} \right) \right] ds_{\Gamma_2}, \tag{27}$$

where

$$p_{x_{2i}} = -\sigma_{2i}, \tag{28}$$

$$p_{y_{2i}} = 0, \tag{29}$$

$$ds_{\Gamma_2} = dz_2, \tag{30}$$

$$\cos\alpha_{\Gamma_2} = -1, \tag{31}$$

$$\frac{\partial u}{\partial x_{\Gamma_2}} = \varepsilon = \kappa_2 \left(z_2 - z_{2n_2}\right). \tag{32}$$

The J-integral in segment, Γ_3, is expressed as

$$J_{\Gamma_3} = \sum_{i=1}^{i=n} \int_{s_{3i}} \left[u_{03i} \cos\alpha_{\Gamma_3} - \left(p_{x_{3i}} \frac{\partial u}{\partial x}_{\Gamma_3} + p_{y_{3i}} \frac{\partial v}{\partial x_{\Gamma_3}} \right) \right] ds_{\Gamma_3}. \tag{33}$$

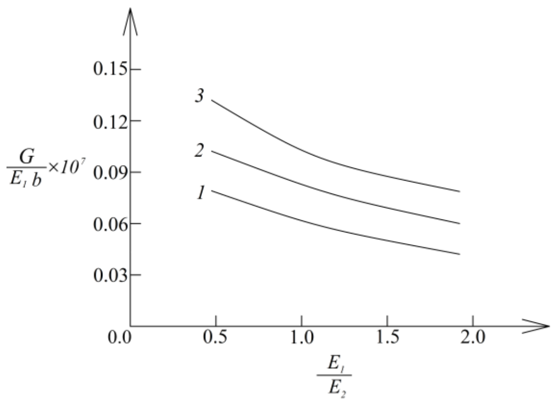

Fig. 5 The strain energy release rate in non-dimensional form plotted against E_2/E_1 ratio (curve 1 - at M=6 Nm, curve 2 - at M=8 Nm and curve 3 - at M=10 Nm)

The components of J_{Γ_3} are found as

$$p_{x_{3i}} = \sigma_{3i}\,, \tag{34}$$

$$p_{y_{3i}} = 0\,, \tag{35}$$

$$ds_{\Gamma_3} = -dz_3\,, \tag{36}$$

$$\cos\alpha_{\Gamma_3} = 1\,, \tag{37}$$

$$\frac{\partial u}{\partial x_{\Gamma_3}} = \varepsilon = \kappa_3\left(z_3 - z_{3n_3}\right). \tag{38}$$

By substituting of (21), (27) and (33) in (20), one arrives at

$$\begin{aligned} J = 2\Bigg\{ &\sum_{i=1}^{i=n_1} \int_{s_{1i}} \left[u_{01i}\cos\alpha_{\Gamma_1} - \left(p_{x_{1i}} \frac{\partial u}{\partial x_{\Gamma_1}} + p_{y_{1i}} \frac{\partial v}{\partial x_{\Gamma_1}} \right) \right] ds_{\Gamma_1} + \\ &+ \sum_{i=1}^{i=n_2} \int_{s_{2i}} \left[u_{02i}\cos\alpha_{\Gamma_2} - \left(p_{x_{2i}} \frac{\partial u}{\partial x_{\Gamma_2}} + p_{y_{2i}} \frac{\partial v}{\partial x_{\Gamma_2}} \right) \right] ds_{\Gamma_2} + \\ &+ \sum_{i=1}^{i=n} \int_{s_{3i}} \left[u_{03i}\cos\alpha_{\Gamma_3} - \left(p_{x_{3i}} \frac{\partial u}{\partial x_{\Gamma_3}} + p_{y_{3i}} \frac{\partial v}{\partial x_{\Gamma_3}} \right) \right] ds_{\Gamma_3} \Bigg\}. \end{aligned} \tag{39}$$

The integration in (39) is performed by using the MatLab computer program. The fact that the J-integral value obtained by (39) matches exactly the strain energy release rate found by (19) is a verification of the delamination analysis of the multilayered frame structure subjected to creep.

3. Parametric study

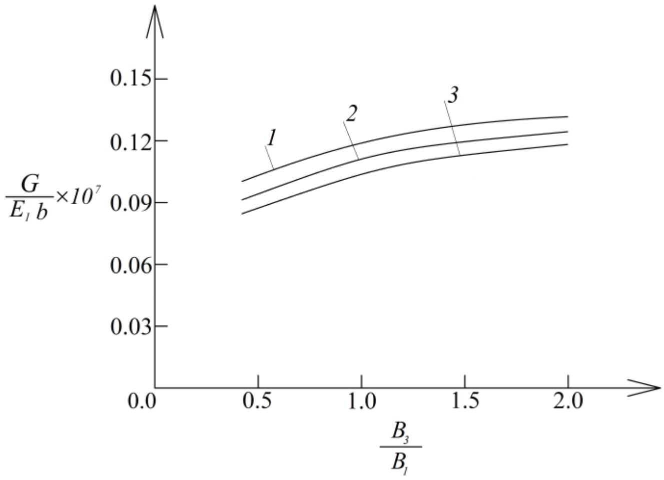

Fig. 6 The strain energy release rate in non-dimensional form plotted against B_3/B_1 ratio (curve 1 - at h/b=1.5, curve 2 - at h/b=1.7 and curve 3 - at h/b=1.9)

In this section of the paper, results of a parametric study of the delamination in the multilayered frame shown in Fig. 1 are presented.

For this purpose, the solution to the strain energy release rate (19) is applied. The strain energy release rate is expressed in non-dimensional form by using the equation $G_N=G/(E_1b)$. In order to evaluate the effect of the delamination crack location in the thickness direction on the delamination fracture behavior of the frame, two three-layered frame configurations are analyzed (Fig. 3). A delamination crack is located between layers 2 and 3 (the adhesion between layers 1 and 2 is perfect i.e., there is no bond deformation between these layers) in the frame configuration depicted in Fig. 3a. A fame configuration with a delamination between layers 1 and 2 is also studied as shown in Fig. 3b (in this case, there is no bond deformation between layers 2 and 3). The thickness of the layers is q in both frame configurations (Fig. 3). It is assumed that q=0.006 m, b=0.012 m and M=10 Nm.

The influence of the time on the delamination behavior is studied. For this purpose, the strain energy release rate in non-dimensional form is plotted against the non-dimensional time in Fig. 4 for the two three-layered frame configurations shown in Fig. 3. The time is expressed in non-dimensional form by using the equation $t_n=t\beta_1$. The cures in Fig. 4 indicate that the strain energy release rate increases with the time due to the creep. It can also be observed in Fig. 4 that the strain energy release rate obtained for the case when the delamination crack is located between layers 2 and 3 is higher in comparison with the strain energy release rate found when the delamination is between layers 1 and 2.

The effect of E_2 in layer 2 of the frame on the delamination is also studied. For this purpose, calculations of the strain energy release rate are carried-out at various E_2/E_1 ratios. The frame configuration with a delamination crack located between layers 2 and 3 is considered (Fig. 3(a)). The results obtained are illustrated in Fig. 5 where the strain energy release rate in non-dimensional form is plotted against E_2/E_1 ratio at thee values of the bending moment, M. It is evident from Fig. 5 that the strain energy release rate decreases with increasing of E_2/E_1 ratio. One can observe also in Fig. 5 that an increase of M causes increases of the strain energy release rate.

The influence of B_3 in layer 3 on the delamination behavior is investigated by performing calculations of the strain energy release rate at various B_3/B_1 ratios.

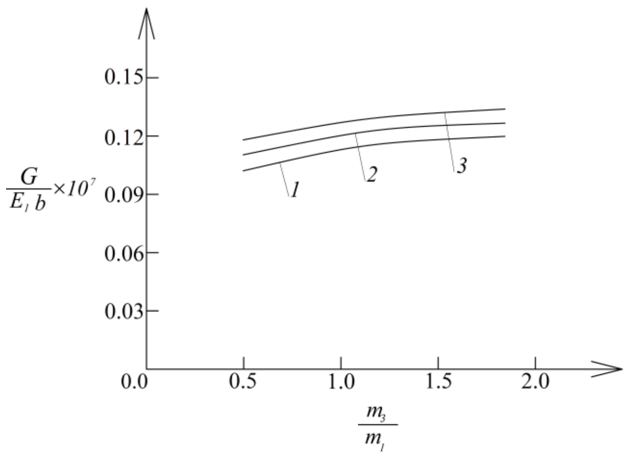

Fig. 7 The strain energy release rate in non-dimensional from plotted against m_2/m_1 ratio (curve 1 - at D_2/D_1=0.5, curve 2 - at D_2/D_1=1.0 and curve 3 - at D_2/D_1=2.0)

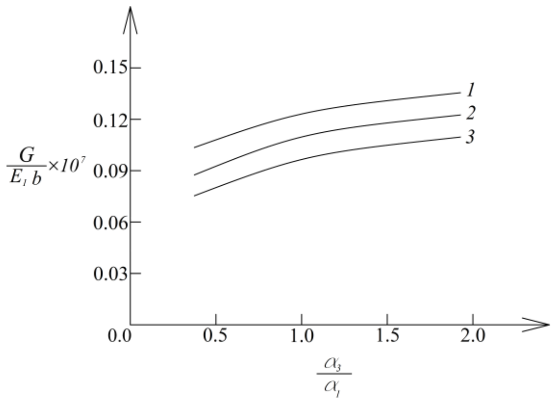

Fig. 8 The strain energy release rate in non-dimensional form plotted against α_3/α_1 ratio (curve 1 - at E_3/E_1=0.5, curve 2 - at E_3/E_1=1.0 and curve 3 - at E_3/E_1=2.0)

The three-layered frame with a delamination located between layers 2 and 3 is analyzed. One can get an idea about the influence of B_3 on the delamination from Fig. 6 where the strain energy release rate in non-dimensional form is plotted against B_3/B_1 ratio at three *h/b* ratios. One can observe in Fig. 6 that the strain energy release rate increases with increasing of B_3/B_1 ratio. The curves in Fig. 6 show that the strain energy release rate decreases with increasing of *h/b* ratio.

The variation of the strain energy release rate with increasing of m_2/m_1 and D_2/D_1 ratios is analyzed. The three-layered frame configuration with a delamination crack located between layers 2 and 3 is considered. The results of the analysis are shown in Fig. 7 where the strain energy release rate in non-dimensional from is plotted against m_2/m_1 ratio at three D_2/D_1 ratios. One can observe in Fig. 7 that the strain energy release rate increases with increasing of m_2/m_1 and D_2/D_1 ratios.

An investigation of the influence of α_3/α_1 ratio on the delamination behavior is performed. The three-layered frame with delamination between layers 2 and 3 is studied. The strain energy release rate is calculated at various α_3/α_1 ratios. The results of these calculations are illustrated in Fig. 8 where the strain energy release rate in non-dimensional form is plotted against α_3/α_1 ratio at three

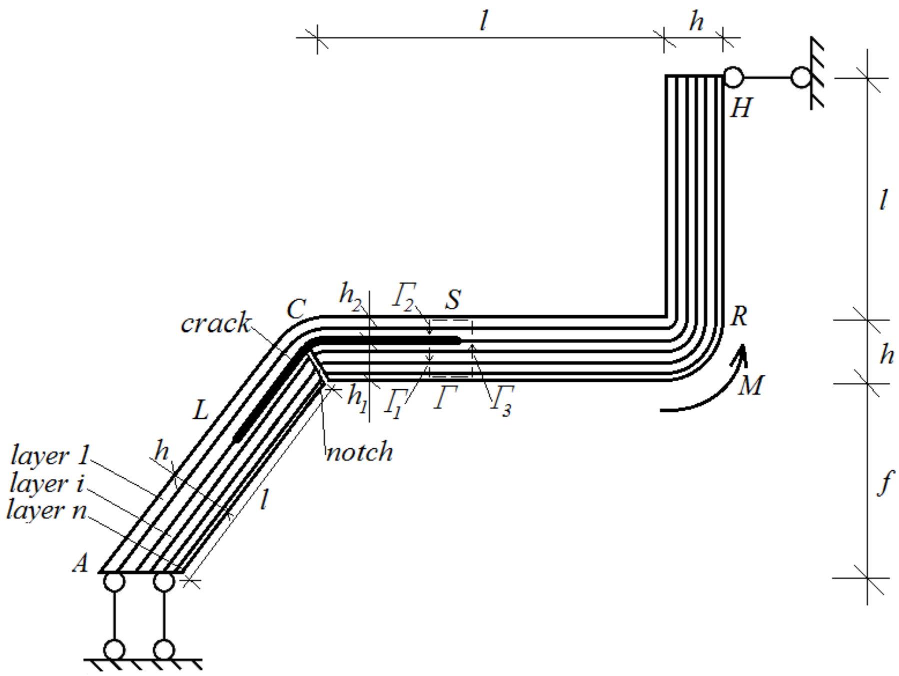

Fig. 9 Geometry and loading of a multilayered frame configuration with a notch in the inner crack arm

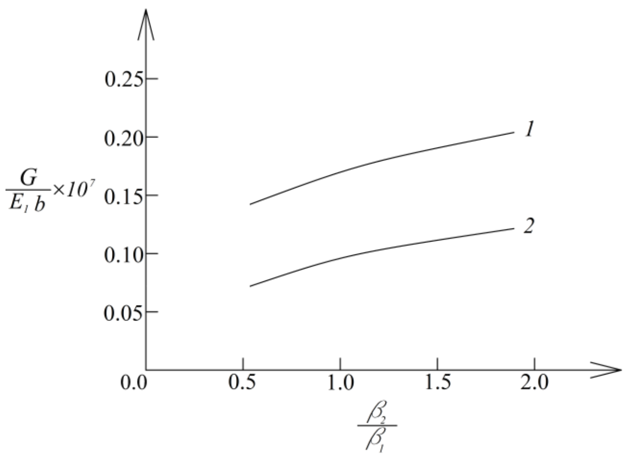

Fig. 10 The strain energy release rate in non-dimensional form plotted against β_2/β_1 ratio (curve 1 - for the multilayered frame with a notch in the inner delamination crack arm, curve 2 - for the multilayered frame without a notch)

E_3/E_1 ratios. The curves in Fig. 8 show that the strain energy release rate increases with increasing of α_3/α_1 ratio. The increase of E_3/E_1 ratio induces decrease of the strain energy release rate (Fig. 8).

The strain energy release rate is derived also for the case when a notch is cut-out in the inner delamination crack arm in C as shown in Fig. 9. In this case, the inner crack arm is free of stresses. Therefore, the complementary strain energy in the inner arm is zero and the solution to the strain energy release rate (19) is re-written as

$$G = \frac{2}{b}\left(\sum_{i=1}^{i=n_2} \iint_{(A_i)} u^*_{02i} dA - \sum_{i=1}^{i=n} \iint_{(A_i)} u^*_{03i} dA \right). \tag{40}$$

The complementary strain energy density in the outer crack arm, u^*_{02i}, that is involved in (40) is found by replacing of σ_{1i} with σ_{2i} in (8).

The curvature and the coordinate of the neutral axis of the outer crack arm cross-section are determined by using the equations for equilibrium (13) and (14) where, in this case, $M_2=M$ since the inner crack arm is free of stresses.

The solution to the strain energy release rate (40) is verified by applying the *J*-integral approach. The integral is solved along the integration contour, Γ, shown by a dashed line in Fig. 9. Since the inner crack arm is free of stresses, $J_{\Gamma_1} = 0$. Therefore, the *J*-integral solution (39) is re-written as

$$J = \sum_{i=1}^{i=n_2} \int_{s_{2i}} \left[u_{02i} \cos\alpha_{\Gamma_2} - \left(p_{x_{2i}} \frac{\partial u}{\partial x}_{\Gamma_2} + p_{y_{2i}} \frac{\partial v}{\partial x_{\Gamma_2}} \right) \right] ds_{\Gamma_2} +$$
$$+ \sum_{i=1}^{i=n} \int_{s_{3i}} \left[u_{03i} \cos\alpha_{\Gamma_3} - \left(p_{x_{3i}} \frac{\partial u}{\partial x}_{\Gamma_3} + p_{y_{3i}} \frac{\partial v}{\partial x_{\Gamma_3}} \right) \right] ds_{\Gamma_3} \Bigg\}. \tag{41}$$

It should be mentioned that the *J*-integral value obtained by (41) is exact match to the strain energy release rate found by (40). This fact verifies the solution to the strain energy release rate for the delamination crack in the multilayered frame configuration with a notch in the inner delamination crack arm (Fig. 9).

The strain energy release rate for the frame configuration with a notch in the inner delamination crack arm is compared to that for the frame without notch in Fig. 10 where the strain energy release rate in non-dimensional form is plotted against β_2/β_1 ratio. The frame with a delamination crack located between layers 2 and 3 is considered. One can observe in Fig. 10 that the strain energy release rate in the multilayered frame with a notch is higher than that in the multilayered frame without a notch. The curves shown in Fig. 10 indicate also that the strain energy release rate increases with increasing of β_2/β_1 ratio.

4. Conclusions

Delamination in a multilayered frame structure that exhibits non-linear creep behavior is analyzed in terms of the strain energy release rate. The frame is made of arbitrary number of adhesively bonded layers with different thicknesses and material properties. A delamination is located arbitrary between layers. Thus, the delamination crack arms have different thicknesses. The time-dependent mechanical behavior of the material in the frame layers is treated by using a non-linear stress-strain-time relationship. A solution to the strain energy release rate is obtained by analyzing the complementary strain energy. The solution to the strain energy release rate obtained in the present paper is time-dependent since a stress-strain-time relationship is used. The delamination is studied also by applying the *J*-integral approach in order to verify the solution to the strain energy release rate. The variation of the strain energy release rate with the time is investigated. It is found that the strain energy release increases with the time. This finding is attributed to the non-linear creep. The effect of the location of the delamination crack along the thickness is evaluated. For this purpose, two three-layered frame configurations are considered. The analysis reveals that the strain energy release rate for the frame configuration in which the inner delamiantion crack arm consists of one layer is higher compared to that for the frame configuration in which the inner delamination crack arm is of two layers. It is found that the strain energy release rate decreases with increasing of E_2/E_1 ratio. The increase of h/b ratio also leads to decrease of the strain energy release rate. Concerning the influence of B_3/B_1, m_2/m_1, D_2/D_1, α_3/α_1 and β_2/β_1 ratios, the study indicates that the strain energy release rate increases with increasing of these ratios. The strain energy release rate is analyzed also for the case when a notch is cut-out in the inner delamination crack arm. The results are compared with these obtained for the case of a frame without a notch. It is found that the strain energy release rate for a frame with a notch in the inner delamination crack arm is higher than that for a frame without a notch. The approach developed in the present paper may be used in fracture mechanics based preliminary structural design of multilayered frames which exhibit non-linear creep behavior.

Acknowledgments

This study was performed during the German Academic Exchange Organization (DAAD) supported research stay of the first author (V.I.R.) in Department of Engineering Mechanics, Institute of Mechanics, Otto-von-Guericke-University, Magdeburg, Germany.

References

Amenzadeh, R.Y. and Kiyasbeyli, E.T. (2007), “Critical time of a long multilayer viscoelastic shell”, *Mech. Compos. Mater.*, **43**(5), 419-426. https://doi.org/10.1007/s11029-007-0039-6.

Amenzadeh, R.Y., Kiyasbeyli, E.T. and Fatullaeva, L.F. (2006), “The limiting state of a rigidly fixed nonlinearly elastic multilayer rod”, *Mech. Compos. Mater.*, **42**(3), 243-252. https://doi.org/10.1007/s11029-006-0034-3.

Amenzadeh, R.Y., Kiyasbeyli, E.T. and Fatullayeva, L.F. (2011), “Flattening of a long multilayered viscoelastic cylindrical shell with a varying wall thickness”, *Mech. Compos. Mater.*, **47**(2), 239-250. https://doi.org/10.1007/s11029-011-9201-2.

Araki, N., Makino, A., Ishiguro, T. and Mihara, J. (1992), “An analytical solution of temperature response in multilayered materials for transient methods”, *Int. J. Thermophys.*, **13**(3), 515-538. https://doi.org/10.1007/BF00503887.

Ariga, K., Ji, Q., Hill, J.P., Bando, Y. and Aono, M. (2012), “Forming nanomaterials as layered functional structures toward materials nanoarchitectonics”, *NPG Asia Mater.*, **4**(5), 1-11. https://doi.org/10.1038/am.2012.30.

Broek, D. (1982), *Elementary Engineering Fracture Mechanics*, Springer, Netherlands.

Cilli, A. and Ozturk, A. (2010), “Dispersion of torsional waves in initially stressed multilayered circular cylinders”, *Mech. Compos. Mater.*, **46**, 227-236. https://doi.org/10.1007/s11029-010-9141-2.

Dowling, N.E. (2013), *Mechanical Behavior of Materials*, Pearson.

Kaul, A.B. (2014), “Two-dimensional layered materials: Structure, properties, and prospects for device applications”, *J. Mater. Res.*, **29**(3), 348-361. https://doi.org/10.1557/jmr.2014.6.

Lloyd, S.J. and Molina-Aldareguia, J.M. (2003), “Multilayered materials: a palette for the materials artist”, *Phil. Trans. R. Soc. Lond. A*, **361**(1813), 2931-294. https://doi.org/10.1098/rsta.2003.1276.

Maraş, S., Yaman, M. and Şansveren, M.F. (2019), “Dynamic analysis of laminated syntactic foam beams”,

3rd International Conference on Advanced Engineering Technologies (ICADET), September.
Maraş, S., Yaman, M., Şansveren, M.F. and Reyhan, S.K. (2018), "Free vibration analysis of fiber metal laminated straight beam", *Open Chem*., **16**, 944-948. https://doi.org/10.1515/chem-2018-0101.
Ozturk, A. (2017), "Propagation of torsional waves in pre-stretched composite cylinder with an imperfect interface", *AIP Conf. Proc.*, **1815**(1), 140004. https://doi.org/10.1063/1.4976492.
Ozturk, A. and Akbarov, S.D. (2009), "Torsional wave dispersion relations in a pre-stressed bi-material compounded cylinder", *ZAMM J. Appl. Math. Mech./Zeitschrift für Angewandte Mathematik und Mechanik*, **89**(9), 754-766. https://doi.org/10.1002/zamm.200800201.
Rizov, V. and Altenbach, H. (2020), "Longitudinal fracture analysis of inhomogeneous beams with continuously varying sizes of the cross-section along the beam length", *Frattura ed Integrità Strutturale*, **53**, 38-50. https://doi.org/10.3221/IGF-ESIS.53.04.
Rizov, V.I. (2017), "Analysis of longitudinal cracked two-dimensional functionally graded beams exhibiting material non-linearity", *Frattura ed Integrità Strutturale*, **41**, 498-510. https://doi.org/10.3221/IGF-ESIS.41.61.
Rizov, V.I. (2018), "Analysis of cylindrical delamination cracks in multilayered functionally graded non-linear elastic circular shafts under combined loads", *Frattura ed Integrità Strutturale,* **46**, 158-177. https://doi.org/10.3221/IGF-ESIS.46.16.
Rizov, V.I. (2019), "Influence of material inhomogeneity and non-linear mechanical behavior of the material on delamination in multilayered beams", *Frattura ed Integrità Strutturale*, **47**, 468-481. https://doi.org/10.3221/IGF-ESIS.47.37.
Rizov, V.I. (2020), "Inhomogeneous multilayered beams of linearly changing width: a delamination analysis", *IOP Conf. Ser.: Mater. Sci. Eng.*, **739**(1), 012004. https://doi.org/10.1088/1757-899X/739/1/012004.
Rizov, V.I. (2020a), "Investigation of two parallel lengthwise cracks in an inhomogeneous beam of varying thickness", *Couple. Syst. Mech.*, **9**(4), 381-396. https://doi.org/10.12989/csm.2020.9.4.381.
Rizov, V.I. (2021), "Delamination analysis of multilayered beams exhibiting creep under torsion", *Couple. Syst. Mech.*, **10**(4), 317-331. https://doi.org/10.12989/csm.2021.10.4.317.
Şansveren, M.F. and Yaman, M. (2019), "The effect of carbon nanofiber on the dynamic and mechanical properties of Epoxy/Glass microballoon syntactic foam", *Adv. Compos. Mater.*, **28**(6), 561-575. https://doi.org/10.1080/09243046.2019.1610929.
Shestov, V.V., Antipov, V.V. and Ryabov, D.K. (2017), "Corrosion resistance and mechanical properties of layered structural material based on aluminum alloy and fiberglass thin sheets", *Metallurgist.*, **60**, 1191-1196. https://doi.org/10.1007/s11015-017-0428-6.
Tekalur, S.A., Shukla, A. and Shivakumar, K. (2008), "Blast resistance of polyurea based layered composite materials", *Compos. Struct.*, **84**, 271-281. https://doi.org/10.1016/j.compstruct.2007.08.008.
Tench, D.M. and White, J.T. (1991), "Tensile properties of nanostructured Ni-Cu multilayered materials prepared by electrodeposition", *J. Electrochem. Soc.*, **138**, 3757-3758.
Wang, X., Sun, Y. and Liu, K. (2019), "Chemical and structural stability of 2D layered materials", *2D Mater.*, **6**, 042001. https://doi.org/10.1088/2053-1583/ab20d6.

AI